Materials Today Bio 13 (2022) 100194

Contents lists available at ScienceDirect

Materials Today Bio

journal homepage: www.journals.elsevier.com/materials-today-bio

Immunomodulatory functions of human mesenchymal stromal cells are enhanced when cultured on HEP/COL multilayers supplemented with interferon-gamma

Mahsa Haseli [a,1], David A. Castilla-Casadiego [a,b,1], Luis Pinzon-Herrera [a], Alexander Hillsley [b], Katherine A. Miranda-Munoz [c], Srikanth Sivaraman [c], Adrianne M. Rosales [b], Raj R. Rao [c], Jorge Almodovar [a,*]

[a] Ralph E. Martin Department of Chemical Engineering, University of Arkansas, 3202 Bell Engineering Center, Fayetteville, AR, 72701, USA
[b] Mcketta Department of Chemical Engineering, The University of Texas at Austin, Austin, TX, 78712, USA
[c] Department of Biomedical Engineering, College of Engineering, University of Arkansas, Fayetteville, AR, 72701, USA

ARTICLE INFO

Keywords:
Layer-by-Layer
Human mesenchymal stromal cells
Collagen
Heparin
Interferon gamma

ABSTRACT

Human mesenchymal stromal cells (hMSCs) are multipotent cells that have been proposed for cell therapies due to their immunosuppressive capacity that can be enhanced in the presence of interferon-gamma (IFN-γ). In this study, multilayers of heparin (HEP) and collagen (COL) (HEP/COL) were used as a bioactive surface to enhance the immunomodulatory activity of hMSCs using soluble IFN-γ. Multilayers were formed, via layer-by-layer assembly, varying the final layer between COL and HEP and supplemented with IFN-γ in the culture medium. We evaluated the viability, adhesion, real-time growth, differentiation, and immunomodulatory activity of hMSCs on (HEP/COL) multilayers. HMSCs viability, adhesion, and growth were superior when cultured on (HEP/COL) multilayers compared to tissue culture plastic. We also confirmed that hMSCs osteogenic and adipogenic differentiation remained unaffected when cultured in (HEP/COL) multilayers in the presence of IFN-γ. We measured the immunomodulatory activity of hMSCs by measuring the level of indoleamine 2,3-dioxygenase (IDO) expression. IDO expression was higher on (HEP/COL) multilayers treated with IFN-γ. Lastly, we evaluated the suppression of peripheral blood mononuclear cell (PBMC) proliferation when co-cultured with hMSCs on (HEP/COL) multilayers with IFN-γ. hMSCs cultured in (HEP/COL) multilayers in the presence of soluble IFN-γ have a greater capacity to suppress PBMC proliferation. Altogether, (HEP/COL) multilayers with IFN-γ in culture medium provides a potent means of enhancing and sustaining immunomodulatory activity to control hMSCs immunomodulation.

1. Introduction

Human mesenchymal stromal cells (hMSCs) are of particular interest for cellular therapy programs [1]. During tissue damage, hMSCs have the ability to secrete paracrine and anti-inflammatory factors to repair tissue [3,4]. In addition, hMSCs contribute not only to the repair of damaged tissues but also possess remarkable immunomodulatory activity by producing anti-inflammatory and immunosuppressive factors [5–10]. Therefore, hMSCs have become apparent as a promising implement for new medical applications and therapies for the treatment of diverse diseases and disorders, such as graft-versus-host disease, inflammatory diseases, and autoimmune disorders [11,12]. Immunosuppression by hMSCs appears as a multifactorial process that relies on cell-cell contact working in collaboration with the secretion of paracrine factors and extracellular vesicles (EVs) [13,14]. However, some studies showed that the immunosuppressive properties of hMSCs are more affected by paracrine mediators rather than cell-cell contact [15,16]. Paracrine mediators (e.g., cytokines, chemokines, and growth factors) modulate the hMSCs microenvironment and influence the activity of resident cells [17]. These specific immune factors, including, interferon-gamma (IFN- γ), tumor necrosis factor-alpha (TNF-α), and interleukin 1 beta (IL-1β), initiate the hMSCs immunosuppression program by inducing the synthesis of protein

* Corresponding author.
E-mail address: jlalmodo@uark.edu (J. Almodovar).
[1] M.H. and D. A. C-C. contributed equally.

https://doi.org/10.1016/j.mtbio.2021.100194
Received 8 November 2021; Received in revised form 20 December 2021; Accepted 22 December 2021
Available online xxxx

factors, in particular indolamine-2,3-dioxygenase (IDO) and inducible nitric oxide synthase [18–20]. It has been shown that the immunosuppressive properties of hMSCs relies on the existence of IFN-γ in the microenvironment [21]. IFN-γ is a potent pro-inflammatory cytokine produced by $CD4^+$ lymphocytes, natural killer cells, and macrophages. It plays essential and complex roles in innate and adaptive immune responses against viral infections, bacteria, protozoa, and graft-versus-host disease (GVHD) [22,23]. However, our group and others have shown that IFN-γ has a significant anti-proliferative effect on hMSCs [12,24].

To overcome these limitations, polymeric biomaterials are engineered to enhance the survival, manufacturing efficiency, and delivery of hMSCs [25,26]. However, the function of polymeric biomaterials is correlated to the donor-donor variability of hMSCs [27,28]. In our previous work done by D. Castilla-Casadiego et al., bone-marrow-derived hMSCs were used to evaluate cell adhesion, proliferation, and cytokine expression on polyelectrolyte multilayers composed of heparin and collagen (HEP/COL) terminating in COL (12 layers HEP/COL) or HEP (13 layers HEP/COL) with IFN-γ supplementation in the culture medium [12]. We demonstrated that the use of (HEP/COL) multilayers is likely to improve the anti-proliferative effect of IFN-γ [12]. In addition, in the work of Cifuentes et al. we evaluated the impact of HEP/COL multilayers on the growth, morphology, and secretome of bone marrow and adipose derived hMSCs [29]. The results of study by Cifuentes et al. suggested that HEP terminated layers are likely to increase hMSC potency under reduced serum conditions. While our previous work suggests that the immunosuppressive properties of hMSCs cultured on HEP/COL multilayers are enhanced in the presence of soluble IFN-γ, we have not directly confirmed this. Thus, this manuscript directly evaluates the immunosuppressive properties of hMSCs cultured on HEP/COL multilayers both by measuring IDO function and suppression of peripheral blood mononuclear cell (PBMC) proliferation using hMSCs from different donors.

The layer-by-layer (LbL) deposition of polyelectrolytes provides compositional uniqueness of natural or synthetic polymers, such as stimulating a specific signal to cells and enhancing cellular behavior [30]. LbL involves the alternative absorption of polycations and polyanions to produce films with specific and controlled physical−chemical characteristics by adapting the experimental parameters, such as pH, ionic strength, and polyelectrolyte concentration [31–33]. Type I collagen is a major fibrous protein in the extracellular matrix (ECM) of connective tissues which interact with cells and other ECM molecules to generate and maintain tissue form and function [34,35]. Furthermore, heparin is a highly sulfated glycosaminoglycan that contains negatively charged carboxylate or sulfate groups present in the ECM and surface of cells [36,37]. Heparin has the ability to bind ECM proteins, such as collagen and thus plays an important role in organizing the structure and composition of the ECM.

Here, we continued our previous work to evaluate the immunomodulatory of two different donors of hMSCs-derived from bone marrow on polymeric multilayers composed of collagen (COL) and heparin (HEP) that are either terminated in COL (12 layers of HEP/COL) or HEP (13 layers of HEP/COL). The reason that we evaluated 12 and 13 layers of HEP/COL is related to our previous work where we showed that there is no differences on cell function as a function of number of layers after 12 layers [29]. We also have previously demonstrated that 12 layers is the minimum number of layers to provide complete surface coverage [38]. These heparin/collagen arrangements will be noted as COL-ending and HEP-ending, respectively. The experiments were conducted for cases with and without IFN-γ as a supplement in the culture medium. The ability of polymeric multilayers, supplemented IFN- γ to induce sustained immunomodulatory activity, was evaluated by measuring IDO expression and PBMC proliferation suppression. In this study, hMSCs growth, viability, differentiation, immunophenotype, and suppression of PBMC proliferation were evaluated as a function of polymeric multilayer composition in the presence or absence of soluble IFN-γ. This study demonstrates that the LbL coating did not negatively influence the viability, adhesion, and differentiation of hMSCs. Moreover, this study shows that hMSCs cultured on (HEP/COL) multilayers supplemented with IFN-γ have a greater capacity to suppress PBMC proliferation. Altogether, this study shows that (HEP/COL) multilayers can modulate a hMSCs response to soluble factors, which may lead to manufacturing and hMSCs-based therapies.

2. Materials and methods

2.1. (HEP/COL) multilayers fabrication

(HEP/COL) multilayers were constructed as described in our previous works [12,29,39,40]. Heparin sodium (HEP) purchased from Celsus Laboratories, Inc. (Cat. #PH3005) and lyophilized type I collagen sponges (COL) derived from bovine tendon (generously donated by Integra Lifesciences Holdings Corporation, Añasco, PR) were used to construct thin polymeric multilayers by the LbL technique on sterile tissue culture-treated plates from Corning Costar (Cat. #07-200- 740). Poly(ethylenimine) (PEI) (50% solution in Water, Mw ≈ 750,000) from Sigma-Aldrich (Cat. #P3143) was used to produce a strong anchoring layer prior to (HEP/COL) multilayers fabrication. All polymer solutions were prepared at a concentration of 1.0 mg/mL in sodium acetate buffer (0.1 M sodium acetate anhydrous, 0.1 M acetic acid, at pH 5 for HEP and PEI, and pH 4 for COL). Sodium acetate buffer at pH 5 was used as washing solution. Ultrapure water at 18 MΩ cm used to prepare polymeric and wash solutions was obtained from a Millipore-Sigma™ Direct-Q™ 3 (Cat. #ZRQSVP3US). Briefly, the process consisted of creating an anchoring layer by depositing PEI solution for 15 min to each well of a sterile tissue culture-treated plate and following with a washing step of 3 min. After this initial step, HEP and COL were added for 5 min alternating with an intermediate wash of 3 min. This process was followed until building a total of 12 polymeric layers of (HEP/COL) (layers ending with COL) and 13 polymeric layers of (HEP/COL) (layers ending with HEP). After preparing the multilayers, a final wash was done using Dulbecco's phosphate-buffered saline (DPBS)1X without Ca^{2+} and Mg^{2+}. Substrates were sterilized using ultraviolet (UV) for 10 min to eliminate any contaminations before cell culture.

2.2. Experimental design

In this work, the effects of the type of surface and the presence or absence of IFN-γ recombinant human protein (ThermoFisher, Cat. #PHC4031) in the culture medium were studied on the cellular response of hMSCs. Three surfaces were assessed; they consisted of a control surface of tissue culture plastic labeled as TCP, a bioactive surface of 12 polymeric layers of (HEP/COL) (layers ending with COL), and 13 layers of (HEP/COL) (layers ending with HEP). IFN-γ supplemented in cell medium, which was added in the cells medium immediately after cell seeding, was evaluated at a concentration of 50 ng/mL, and conditions with and without IFN-γ were designated as + IFN-γ and −IFN-γ, respectively. A 50 ng/mL concentration for soluble IFN-γ was selected based on our previous study [25,26]. Time points and the initial number of cells were selected according to the nature of the specific method used [40].

2.3. Physical characterizations of (HEP/COL) multilayers

Atomic Force Microscope (AFM) images were taken using an Agilent Asylum MFP-3D AFM in contact mode, using a PPP-CONTR-10 (Nano-AndMore, Resonance frequency 6–12 kHz, Force Constant 0.02–0.77 N/m) probe. 80 × 80 μm images were first taken of the dry substrate. The probe was then raised, and phosphate-buffered saline (PBS) was carefully added using a micropipette until both the probe and the substrate were completely submerged. The sample was then hydrated for 5 min to obtain "wet" images.

2.4. In-situ deposition of (HEP/COL) multilayers

The multilayer growth and IFN-γ interaction with the (HEP/COL) were followed by quartz crystal microbalance (QCM-D) with dissipation measurements. QCM-D measurements were performed on a quartz crystal microbalance with dissipation from Biolin Scientific, Sweden. The multilayer build-up process was described in our previous work [40]. Briefly, the quartz crystal was immersed in 5:1:1 (volume parts) at 75 °C of water, 25% ammonia, and 30% hydrogen peroxide. The clean quartz crystal was placed in the QCM-D chamber. Then the PEI solution was injected at a flow rate of 100 mL/min continuously for 15 min. After PEI, a wash with sodium acetate buffer at pH 5 was performed for 3 min at the same flow rate. Then HEP solution was injected at the same rate for 5 min, followed by the same sodium acetate buffer wash at pH 5 for 5 min. After that, the COL solution was injected for 5 min at the same rate, followed by the same sodium acetate buffer wash at pH 5 for 5 min. HEP and COL were then alternately injected into the chamber (followed by the same sodium acetate buffer wash in between each injection). After 12 or 13 multilayers were constructed, IFN-γ in PBS at pH 7.4 was injected into the chamber for 1 h. The frequency shift (-ΔF) and dissipation (ΔD) vs. time curves were recorded.

2.5. Chemical composition of HEP/COL multilayers

The elemental and chemical composition of the multilayers was confirmed by X-ray Photoelectron Spectroscopy (XPS) (Versaprobe XPS from Physical electronics). XPS experiments were performed at a photoelectron takeoff angle of 458 on dry glass substrate, and binding energy scales were referenced to the C1s peak (284.7eV).

2.6. Cell culture

Human bone marrow-derived mesenchymal stem cells purchased from RoosterBio (Cat. #MSC-003), were used between passages 4–6. Donor#1 is a healthy 25-year-old male (Lot. 00174), and donor#2 is a healthy 22-year-old male (Lot. 00178). The product specification sheet provided by the vendor shows that these cells were positive for CD90 and CD166 hMSCs identity markers (as tested by flow cytometry), negative for CD45 and CD34 (as tested by flow cytometry) and could differentiate into fat and bone cells. hMSCs were grown in alpha-minimum essential media MEM Alpha (1 ×) from Gibco (supplemented with L-glutamine, ribonucleosides, and deoxyribonucleosides) (Cat. #12561-056) containing 20% fetal bovine serum from Gibco (Cat. #12662029), 1.2% penicillin-streptomycin from Corning (Cat. #30002CI), and 1.2% L-glutamine from Corning (Cat. #25005CI).

2.7. HMSC viability on (HEP/COL) multilayers

For hMSCs viability, the PrestoBlue™ cell viability assay from Invitrogen (Cat. #A13261) was used. hMSCs (10000 cells/cm^2) were seeded on each surface prepared on a 96 well-plate, and cell viability was measured after 3 days of culture as described in our previous works [29,40]. Briefly, the cell culture medium was removed after 3 days, and 100 μL per well containing 90% fresh cell medium and 10% PrestoBlue reagent were added. The plate was incubated for 3 h, and the fluorescence intensity measurement was determined using a BioTek Multi-Mode Microplate Reader (Model Synergy™ 2) with excitation/emission of 560/590 nm.

2.8. Real-time monitoring of hMSCs behavior on (HEP/COL) multilayers

A Real-Time Cell Analyzer (RTCA) xCELLigence instrument from ACEA Biosciences Inc. (Cat. #380601000) was used to measure real-time cell behavior. (HEP/COL) multilayers were constructed on the wells of an ACEA™ E-Plate L8 (Cat. #300600840, cell growth area of 0.64 cm^2 per well), which are composed of tissue culture plastic, but they also contain sensors to measure impedance, and hMSCs at a concentration of 20000 cells/cm^2 were seeded on each condition evaluated; uncoated sensors, multilayers ending in HEP, and ending in COL with and without IFN-γ supplemented in the culture medium. xCELLigence instrument was configured as described in our previous works [40,41]. Briefly, the xCELLigence RTCA S16 was placed inside the incubator to allow the S16 device to warm up for at least 2 h before use. This step is to avoid any condensation on the station after starting the measurement stage. The RTCA was set up to monitor perform readings every 10 min for a period of 48 h of cell culture.

2.9. Immunomodulatory factor expression of hMSCs on (HEP/COL) multilayers

hMSCs (5000 cells/cm^2) with and without IFN-γ treatment were seeded on each surface prepared on a 24 well-plate. IDO activity was measured after 6 days of culture (changing the cells medium every 2 days) as described in our previous work [41]. Briefly, cell supernatant 100 μL was mixed with 100 μL standard assay mixture consists of (potassium phosphate buffer (50 mM, pH 6.5), ascorbic acid (40 mM, neutralized with NaOH), catalase (200 μg/mL), methylene blue (20 μ M), and L-tryptophan (400 μM)). The mixture was kept at 37 °C in a humidified incubator with 5% CO_2 for 30 min (in a dark environment to protect solutions from light) to allow IDO to convert L-tryptophan to N-formyl-kynurenine. After that, the reaction was stopped by adding 100 μL trichloroacetic acid 30% (wt/vol) and incubated for 30 min at 58 °C. After hydrolysis of N-formyl-kynurenine to kynurenine, 100 μL of mixed cell supernatant/standard transfer into a well of a 96-well microplate, followed by adding 100 μL per well of 2% (w/v) p-dimethylaminobenzaldehyde in acetic acid on each well. Absorbance was read at 490 nm at the endpoint using a BioTek Synergy 2 spectrophotometer (Synergy LX Multi-Mode Reader from BioTek® Model SLXFA). Absorbance readings were converted to concentration of kynurenine using an equation obtained from a calibration curve (plot the absorbance vs. concentration of standard solutions). Amounts of kynurenine were normalized by number of cells per well.

2.10. Peripheral blood mononuclear cells co-culture

For the hMSCs immunosuppressive capacity, human primary peripheral blood mononuclear cells (PBMC), were purchased from ATCC (ATCC® PCS¬800¬011™ Part number: 302213). Briefly, 62500 hMSCs cells/cm^2 with and without IFN-γ treatment were seeded on each surface prepared on a 24 well-plate for 3 days. PBMCs were labeled using a Cell Trace Yellow Cell Proliferation Kit (Invitrogen) at a final dye concentration of 5 mM. Before being added to each well for co-culture, the PBMCs were incubated for 15 min with human T activator CD3/CD28 Dynabeads (Invitrogen) and recombinant human IL-2 (30 U/mL). After this time, the PBMCs and Dynabeads were added to each well to achieve a 1:4 ratio of hMSCs to PBMCs. Based on the study done by Cuerquis et al. the reduction in the percentages of T cells was less significant at a MSC:PBMC ratio of 1:9 compared with 1:3 [13]. In another study, the results showed that a higher ratio of MSC:PBMC was more efficient than a lower ratio [43]. In addition, other studies used the ratio 1:4 for MSC:PBMC for the co-culture experiment [44,45]. In this study, we used the ratio 1:4 to have a better comparison of results with others studies. hMSCs:PBMCs co-cultures were maintained in alpha-minimum essential medium (MEM-alpha) (1) from Gibco, supplemented with L-glutamine, ribonucleosides, and deoxyribonucleosides containing 20% fetal bovine serum from Gibco, 1.2% penicillin-streptomycin from Corning, and 1.2% L-glutamine from Corning for 3 days. After 3 days, the medium from the wells (containing the suspended PBMCs/Dynabeads) was collected into a 1.5 mL tube and protected from light. The tubes were placed in DynaMag magnets from Thermofisher (Cat. #12301D) to remove the Dynabeads. Then, PBMCs were resuspended in MEM-alpha followed by analysis on a BD FACSCanto II flow cytometer to investigate PBMCs proliferation in

the presence and absence of hMSCs and/or IFN-γ cultured on the multilayers and TCP. The data were normalized by using forward scatter (FSC) and side scatter (SSC) parameters to exclude cell debris and aggregates.

2.11. HMSC differentiation stains

hMSCs (5000 cells/cm^2) were seeded on each surface prepared on 24 well-plates and grown for 6 days in expansion medium (MEM Alpha (1) from Gibco (supplemented with L-glutamine, ribonucleosides, and deoxyribonucleosides) containing 20% fetal bovine serum from Gibco, 1.2% penicillin-streptomycin from Corning, and 1.2% L-glutamine from Corning) at 37 °C in a humidified atmosphere of 5% CO_2. After the cells reached at least 50% confluency, they were exposed to osteogenic differentiation medium (DMEM low glucose, 10% fetal bovine serum from Gibco, 1% penicillin, 1% L-Glutamine, 50 μM ascorbic acid (Sigma, Cas Number: 50-81-7) (50 mg/10 mL), 10 mM β-glycerophosphate (e.g., Sigma, CAS Number: 154804-51-0, G9422), 100 nM dexamethasone (e.g., Sigma, CAS Number 50-02-2)), and the medium was replaced every 2–3 days. To maintain the consistency of all experimental design, we seeded the cells with the regular expansion medium for six days. After that we added the differentiation medium for 7–10 days. After culture for one week, cells were fixed with 10% formaldehyde. Alizarin Red S (Sigma, CAS Number 130-22-3) staining solution was prepared by dissolving 2 g of Alizarin Red S in 90 mL distilled water and adjusting the pH to 4.1–4.3 with ammonium hydroxide. Alizarin Red S solution was added, then rinsed with PBS. The sample was analyzed immediately under the microscope to detect calcium deposits. For adipogenic differentiation, an induction medium composed of complete DMEM high glucose supplemented with 10% fetal bovine serum from Gibco, 1% penicillin, 1% L-glutamine, 1 μM dexamethasone (e.g., Sigma, CAS Number 50-02-2), 0.01 mg/mL insulin (Sigma-Aldrich, Catalog No. I2643), 0.5 mM 3-isobutyl-1-methylxanthine (IBMX) (e.g., Sigma, CAS Number: 28822-58-4, I5879), and 100 μM indomethacin (Sigma, CAS Number: 53-86-1) was used. The medium was replaced every 2–3 days. After culture for a week, cells were fixed with 10% formaldehyde, stained with 0.5% (w/v) Oil Red O (Sigma-Aldrich, Catalog Number: O0625) in isopropanol and incubated at room temperature for 10–30 min in the dark, then washed twice with PBS. The sample was observed under a light microscope to determine the number of hMSCs-derived adipocytes.

2.12. Alkaline phosphatase (ALP) assay

To confirm osteogenic differentiation and to determine the level of activity of the differentiated hMSCs, two assays were performed: alkaline phosphatase (ALP) activity and total protein content (micro-BCA assay). Alkaline phosphatase activity was assessed using the Alkaline Phosphatase Colorimetric Assay Kit (Abcam ab83369). According to standard protocols, after the cell's exposure to osteogenic differentiation medium for periods of 3 days, cells were washed twice with PBS. Then, 50 μL of the cell lysate with assay buffer was added to a 96 well-plate and 50 μL p-nitrophenyl phosphate (pNPP). The samples were incubated at 25 °C for 60 min and protected from light. In the last step, 20 μL stop solution was added to the wells, then; the plate was read at 405 nm in a microplate reader (Synergy LX Multi-Mode Reader from BioTek® (Model SLXFA). Alkaline phosphatase (ALP) activity was normalized by total protein content (micro-BCA assay). The total protein content was determined according to the protocol of the manufacture 150 μL of sample was placed in a 96 well-plate with 150 μL of working reagent made from a micro-BCA protein assay kit (Thermo Scientific). The well plate was covered with foil and incubated at 37 °C for 2 h. Absorbance was read at 562 nm using a BioTek Multi-Mode Microplate Reader (Model Synergy™ 2).

2.13. Flow cytometry analysis

Osteogenic and adipogenic cell markers of differentiated hMSCs were analyzed using flow cytometry. hMSCs (25000 cells/cm^2), with and without IFN-γ treatment, were seeded on each surface prepared on a 12 well-plate and expanded using growth medium at 37 °C in a humidified atmosphere 5% CO_2 for 6 days. After the cells reached at least 50% confluency, they were exposed to osteogenic and adipogenic differentiation medium, and the medium was replaced every 2–3 days. Undifferentiated cells grown in expansion media (MEM Alpha) were maintain as control. After 3 days, the cells were detached by trypsinization and washed twice with PBS (centrifuged at 300 g for 10 min). Aliquots were prepared containing 1×10^5 cells in PBS with 2% FBS for staining conjugated primary antibody were incubated against CD105 (PE Mouse anti-Human CD105, BD Biosciences), CD10 (PE Mouse anti-Human CD10, BD Biosciences), and CD92 (Alexa Fluor® 647 Mouse Anti-Human CD92, BD Biosciences). The samples were covered with aluminum foil during the process and incubated at 4 °C for 30 min in the dark. For each type of antibody used, an additional sample with a non-specific isotype control antibody was added. Isotype matched control antibodies PE labeled Mouse IgG1 (BD Pharmingen), and Alexa Fluor® 647 Mouse IgG1 κ Isotype Control (BD Pharmingen) were used for assessment of background fluorescence. The Flow Cytometry analysis was performed using a BD FACS Canto II flow cytometer, using FlowJo software (Tree Star, Oregon, USA) for analysis. At least 10,000 gated events per acquisition were acquired. The median relative fluorescence unit was used for statistical analyses.

2.14. Statistical analysis

The results were presented as mean ± standard deviation. Comparisons among multiple groups were performed by one-way analysis of variance (ANOVA) using Minitab 17 for Windows. A p-value < 0.05 was considered statistically significant.

3. Results and discussion

3.1. Surface characterization

The in-situ assembly deposition of (HEP/COL) multilayers was monitored by QCM-D. QCM-D detects the adsorbed mass of polyelectrolytes (-ΔF) and measures the viscoelastic properties of the surface (ΔD) [46]. QCM-D was used here to investigate physical structures within the multilayer of heparin and collagen. Fig. 1 shows the frequency shift (-ΔF) and dissipation (ΔD) for the third, fifth, and seventh overtones for COL-ending and HEP-ending multilayers. The alternating 3 min of rinsing and 5 min of adsorption steps can be observed. The first 15 min correspond to a PEI step, followed by a 3 min rinsing step in Fig. 1, each physical polyelectrolyte adsorption step is followed by 3 min of rinsing. The increase in -ΔF and ΔD of every (HEP/COL) sequential deposition shows that the polyelectrolytes gradually deposit onto the quartz crystal. This increase can be considered a linear increase of thickness for the multilayers. It is demonstrated that by increasing -ΔF the mass added to the layers increases, whereas the growth of ΔD is due to the enhanced viscoelastic structure of the deposited film [47]. Therefore, adding rough layers on quartz crystal has a shorter -ΔF, whereas a dense layer has a large ΔD value. When collagen is deposited, -ΔF and ΔD have a sharp rise with great dispersion between different overtones in both COL and HEP-ending multilayers [48]. This indicates that the collagen is a loose and swollen layer [48]. In contrast, the heparin deposited shows a slight increase in -ΔF and a decrease in ΔD. These indicated that a rough layer was obtained after the heparin deposition [48]. Our previous study showed that HEP-ending multilayers have higher thickness and

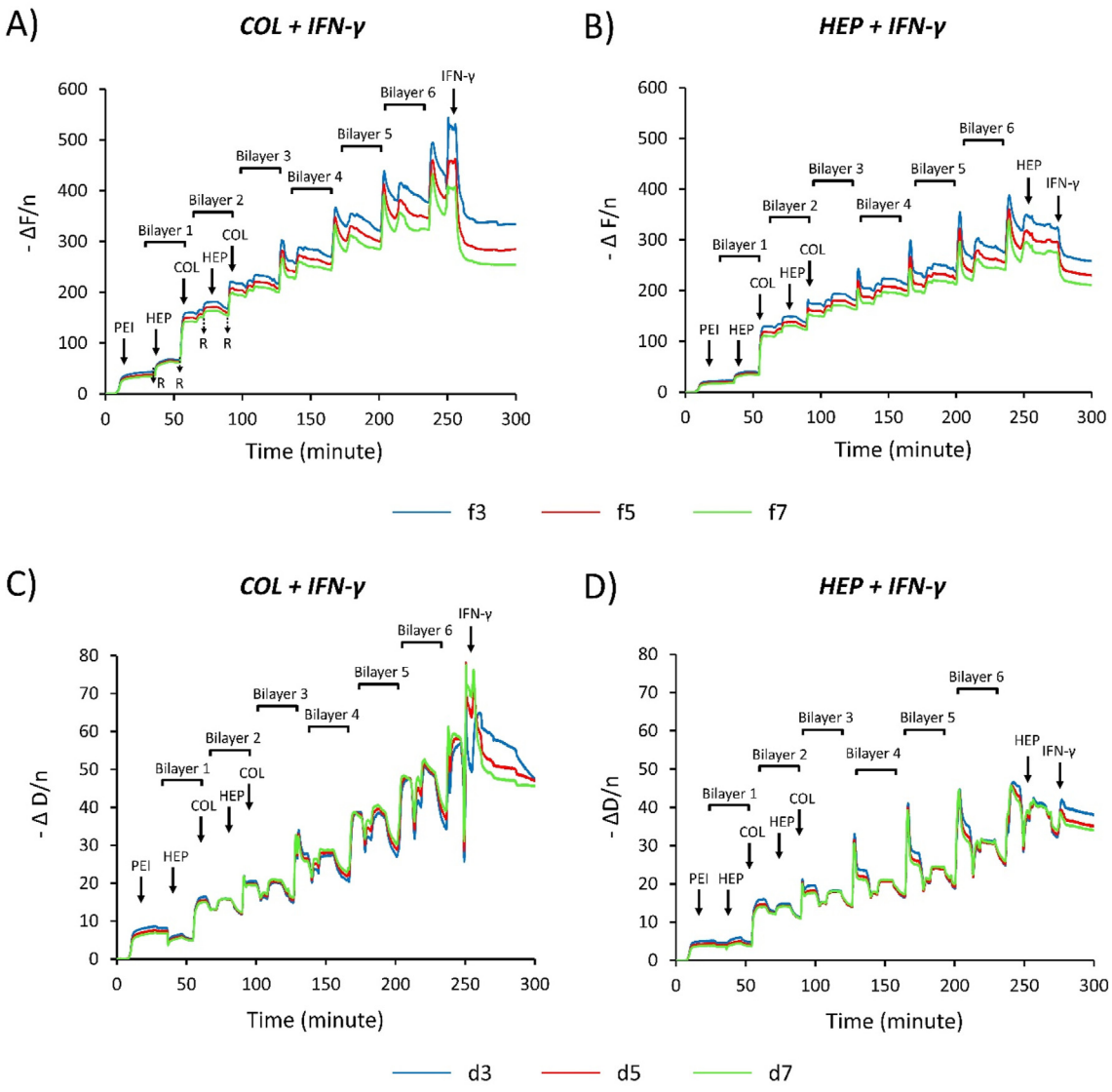

Fig. 1. QCM-D data showing the normalized frequency shift & dissipation shift as a function of time for the 3rd, 5th, and 7th overtones during the construction of the COL ending and HEP ending multilayers with IFN-γ, with alternating 3-min rinse and 5 min adsorption intervals. (A&B): shows the normalized frequency shift. (C&D): shows the normalized dissipation shift.

roughness than the COL-ending multilayers at both 25 °C and 37 °C [12]. In addition, the frequency shifts do not overlap for the different overtones not only in the rinse steps but also during the adsorption steps. Consequently, this indicates that the Sauerbrey relation is not valid for determining the film mass during rinse and adsorption steps, which indicates the film is more viscoelastic. Besides, the ratio of the change during rinse and the adsorption steps in the dissipation factor to the change in frequency ($\Delta D/(-\Delta F/n)$) remain higher than 4×10^{-7} Hz^{-1}; therefore, the film can be considered soft [49]. After adsorption of the IFN- γ, the frequency shifts no longer overlap. This indicates that adsorbed films are viscoelastic and that the mass does not follow the Sauerbrey relationship, so a more complex model might be used to determine the adsorbed mass from the frequency shift and dissipation data [50]. Fig. 1 (A) shows significant frequency shifts following the adsorption of the IFN- γ on the COL-ending multilayers surface for the 3 overtones, indicating that the IFN- γ is strongly adsorbed.

In contrast, Fig. 1 (B) shows the decrease of the frequency shifts following the adsorption of the IFN-γ on the HEP-ending multilayers surface, resulting in negligible adsorption of the IFN-γ. Following adsorption of the IFN- γ, a quick decrease of the frequency shifts are found for both COL-ending and HEP-ending multilayers, which is due to the buffer effect, and the trend levels [51]. These results indicate that the (HEP/COL) multilayers present good stability in presence of the IFN-γ.

The topography of dried and wet (HEP/COL) multilayers was investigated by AFM for COL-ending and HEP-ending multilayers. Analyzing the topographic images in Fig. 2 (A) shows HEP-ending multilayers has larger clusters on the surface, which demonstrate considerable accumulation associated with surface deposition [50]. Also, the deposition of HEP-ending multilayers on dry condition leads to a rougher surface than the COL-ending multilayers. Regarding the wet condition, Fig. 2 (B) shows that the surface has a greater number of smaller clusters on COL-ending than in HEP-ending, demonstrating that the HEP successfully attached to the surface and deposition of HEP may increase roughness of surfaces. These results confirm the conclusions drawn from the QCM-D results in which a rough layer was obtained after HEP deposition in wet conditions. Also, Fig. 2 (A&B) show that the multilayers on dry condition are rougher. However, the multilayers have a smooth surfaces in wet condition which may improve cell adhesion as suggested by Salloum et al. who investigated the combined effects of increasing surface charge and hydrophobicity on vascular smooth muscle cell adhesion [52].

The XPS broad spectra and high-resolution spectra of COL-ending and

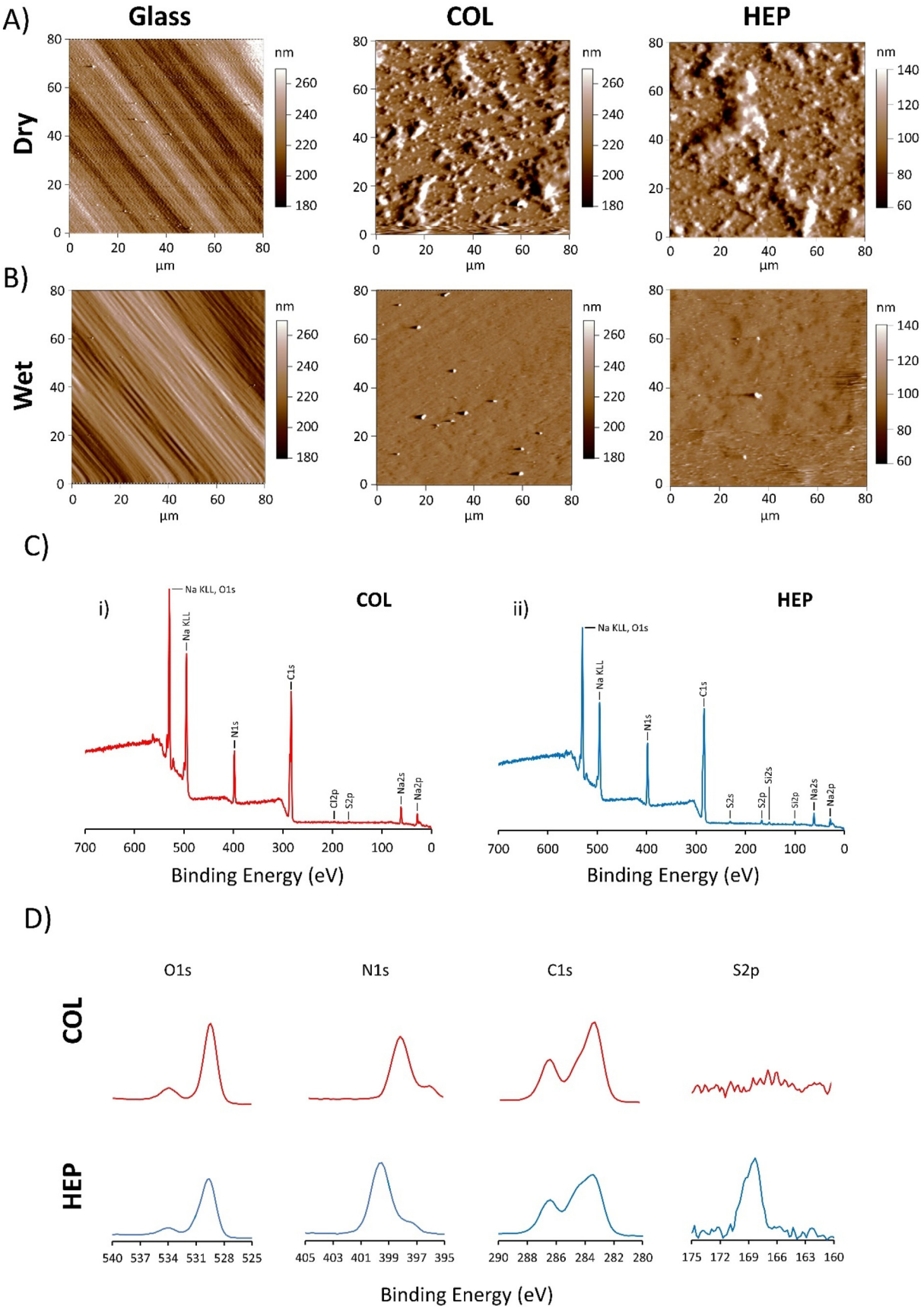

Fig. 2. (A&B) Surface morphology as measured by AFM of: uncoated glass, COL-ending, and HEP-ending multilayers on dry and wet conditions. Chemical properties of (HEP/COL) multilayers as measured by XPS broad spectra and high-resolution XPS. (C): XPS survey scan spectrum of COL-ending, and HEP-ending multilayers. (D): the corresponding specific spectrum of elemental COL-ending, and HEP-ending multilayers.

HEP-ending multilayers are shown in Fig. 2 (C&D). In our previous study, we demonstrated that the thickness of COL-ending multilayers was approximately 129 nm [12]. The XPS could only detect about 10 nm depth of nanometer surface; also, only the outmost layer can be examined from XPS. The XPS spectrum of COL-ending and HEP-ending multilayers contained five peaks corresponding to C1s (283.4 eV), N1s (398.4 eV), O1s (529.8 eV), Na KL1, Na2P, Na2S, and S2P (168.3 eV). Na and S were mainly the characteristic elements of heparin polysaccharide structure possessing $-COO^-$, $-SO_4^{-2}$ and –OH, while collagen contains a large number of various amino acids with $-NH_2$ and –COOH [53]. The presence of more sulfur was detected on the HEP-ending multilayers and revealed the presence of heparin [54]. According to the study of Dan Li et al. [55], collagen has the characteristic sulfur element, but with low content, further demonstrated the successful assembly process. High-resolution spectra of S2p suggested that the surface presented more of S element on HEP-ending multilayers, indicating heparin's presence in the last layer. The increase of sulfur peak due to increasing the number of layers shows a successful deposition of heparin. This finding complies with a previous study by Almodovar et al. [56]. Moreover, oxygen and nitrogen intensity content decrease in HEP-ending multilayers compared to 12 multilayers, indicating that most surfaces of COL-ending multilayers were coated by collagen. In addition, COL-ending multilayers have a higher C1s peak compared to HEP-ending multilayers, including C-C (283.4 eV), C-O, and C–N (286.4 eV) groups. Consequently, a higher carbon, oxygen, and nitrogen content confirm the accumulation of collagen, while heparin deposition shows higher sulfur peaks.

3.2. HMSC viability on (HEP/COL) multilayers

Fluorescence microscopy analysis of cells attached to the different surfaces after 72 h (Fig. 3 (A&A')) reveals that donor#1 and donor#2 hMSCs were well spread, showed a complete confluence and adopted a polygonal morphology on different surfaces. These results indicate that the conditions with (HEP/COL) multilayers with and without IFN-γ do not directly influence cellular phenotype via the organization of cytoskeleton.

The PrestoBlue reagent was used for measuring cell viability after 3 days of culturing cells. A cell density of 15000 cells/cm^2 was used in 96-well plates (working volume of 200 μL). hMSCs were seeded on TCP, COL-ending and HEP-ending multilayers with and without (50 ng/mL) IFN-γ supplemented in the cell culture medium. We selected a concentration of 50 ng/mL for soluble IFN-γ based on our previous study done by D. Castilla-Casadiego et al. [12] and H. Wobma et al. [57]. In the absence of the IFN-γ in culture medium, TCP surfaces were selected as the positive control, and its fluorescence intensity was normalized to 100%. All other conditions were assessed in relation to the positive control. Fig. 3 (B) shows significant differences in the cell viability of donor#1 on COL-ending and HEP-ending multilayers without the IFN-γ compared to the control substrate ($p < 0.05$ and $p < 0.001$, respectively) after 72 h of incubation. However, donor#2 shows that cell viability is not significantly different for substrates containing (HEP/COL) multilayers compared to the control substrate (Fig. 3 (B′)). Also, Fig. 3 (B) indicates that cell viability for donor#1 compared with the TCP surface has an increasing trend. In this regard, there is an approximately 24% increase

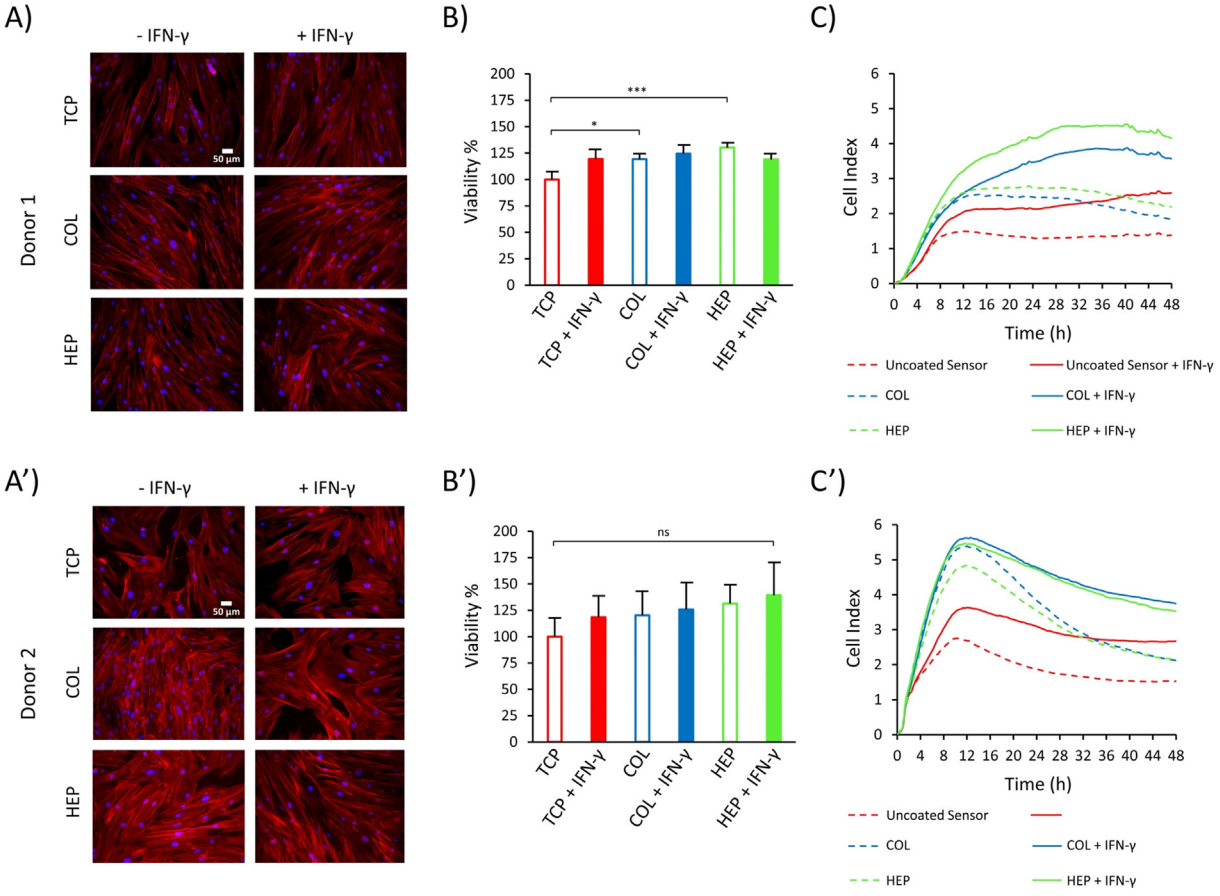

Fig. 3. Fluorescence microscopy images of hMSCs nuclei and actin labeled with Hoechst and Actin Red, respectively, after 3 days of culture for donor#1 (A) and for donor#2 (A′). (B): PrestoBlue Viability assay for hMSCs cultured on TCP, COL-ending, and HEP-ending multilayers with and without IFN-γ for donor#1 (B) and for donor#2 (B′). Real-time monitoring of hMSCs grown on COL-ending, and HEP-ending multilayers during 48 h of culture donor#1 (C) and for donor#2 (C′). Cell cultures were done on multilayers with and without IFN-γ and uncoated sensor was used as control. Data are presented as the mean ± standard deviation of n = 4 samples. The p-values < 0.05 are represented by *, p-values < 0.01 by **, p-values < 0.001 by *** and p-values < 0.0001 by ****.

in cell viability on COL-ending and about a 26% increase in cell viability on HEP-ending in absence of the IFN-γ in culture media. Similarly, donor#2 shows the same result (Fig. 3 (B′)). Therefore, it shows that the use of (HEP/COL) multilayers can increase hMSCs viability. These results indicate that there is a synergistic action of (HEP/COL) multilayers which leads to an increase in cell viability. These results are in line with the results shown in the next section using the real-time cell monitoring system. We observed an increased in cell adhesion and proliferation in the conditions where cells were cultured on (HEP/COL) multilayers (Fig. 3 (C & C')).

In addition, regarding donor#1, despite following the increasing trend of cell viability compared to control substrate (TCP), the cell viability on HEP-ending multilayers with the IFN-γ is less than that of the HEP-ending multilayers without the IFN-γ. However, donor#2 shows that the surfaces with IFN-γ have a higher cell viability than the surfaces without IFN-γ. In particular, HEP-ending multilayers show the highest cell viability (Fig. 3 (B')). Based on our previous study done by D. Castilla-Casadiego et al. [12], hMSCs showed an increase in their proliferation and protein expression when they were grown in multilayers of (HEP/COL) supplemented with IFN-γ. Moreover, Jingchun Du et al. [58] studied the effects of the IFN-γ on the antitumor activity of human amniotic fluid-derived mesenchymal stem cells and revealed that IFN-γ can enhance cell viability. The reason for the superior performance of heparin can be attributed to the fact that heparin has a large binding capacity for several proteins such as tumor necrosis factor-alpha (TNF-α), IFN-γ, and basic fibroblast growth factor (FGF-2), which can modulate cell adhesion and proliferation [59–61]. In fact, in our previous work by D. Castilla-Casadiego we observed an upregulation of FGF-2 expression when hMSCs were cultured on HEP-ending coatings [12]. Thus, (HEP/-COL) multilayers even with and without the IFN-γ, have the ability to improve cell viability.

3.3. Real-time monitoring of cell behavior and proliferation

In this study, we cultured hMSCs at 25000 cells/cm^2 on COL-ending and HEP-ending multilayers to evaluate the real-time behavior of the cells during the first 48 h of culture. The action of IFN-γ in the cell medium was also evaluated. As a control surface, hMSCs cultured on uncoated biosensors was evaluated. The Real-Time Cell Analyzer (RTCA) xCELLigence biosensor system was used, which allows cell proliferation and growth measurement. RTCA xCELLigence constantly measures the impedance difference caused by cells attached to microsensors present in culture plates (E-plates). The schematic of the xCELLigence instrument is shown in Fig. 4. Impedance measurements are translated into a parameter known as the Cell Index (CI). CI is defined as the difference between the background electric resistance (measured using only cell medium) Z0, and the resistance measured at time t in the point i, Zi. The CI value is taken at a frequency of 15Ω. CI values are given by equation 1 [62].

Therefore, the higher the CI, the greater the number of cells adhered to the bottom of the well [39]. Fig. 3 (C) shows the CI values as a function of the first 48 h of culture for the 6 experimental conditions for donor#1. The results show a minor but continuous proliferation until 30 h, followed by a period of stability where the decrease in the curves is very low. It is possible to identify a phase of CI increase that is attributed to the initial stage of cell adhesion. Donor#1 shows a slow cell adhesion stage in the evaluated period, reaching a maximum peak of around 30 h donor#2 shows a negative slope due to cell detachment that occurs after initial adhesion. This behavior is normal for most adherent cells. For donor#2, the cell adhesion stage reached a maximum at 12 h (Fig. 3 (C')). The addition of IFN-γ (at 50 ng/mL) led to a higher CI value for all conditions, with a significant increase on (HEP/COL) multilayers compared to the uncoated sensor. The presence of IFN-γ may increase hMSCs adhesion, which is further amplified in the presence of (HEP/-COL) multilayers [63]. This finding once again confirms that the multilayers improve the response of hMSCs to IFN-γ. In addition, the cultures on (HEP/COL) multilayers (without IFN- γ) also showed better results compared to the controls on uncoated surfaces.

3.4. IDO function

Indoleamine 2,3-dioxygenase (IDO) is a cytosolic heme protein that is vital for cell growth [64]. It can be determined by measuring the amino acid kynurenine in the culture supernatant after 6 days [65]. A cell density of 5000 cells/cm^2 was used in 24-well plates (working volume 600 μL). The ability of IFN-γ to induce IDO function in hMSCs was compared on TCP, COL-ending, and HEP-ending multilayers after 6 days post-stimulation with or without the IFN-γ supplemented in the cell culture medium. The level of IDO is determined by the amount of kynurenine measured (pg/cell), since IDO is known to be a catalyzer to convert L-tryptophan to kynurenine [64]. Results for IDO activity are summarized in Fig. 5 (A), which shows that for donor#1, all surfaces with IFN-γ (including TCP, COL, and HEP) have two times higher levels of the IDO compared to surfaces without IFN-γ (60 pg/cell). Regarding the surfaces with IFN-γ, donor#2 shows significant differences for

$$CI = \frac{(Zi - Z0)}{15\Omega}$$

Equation 1

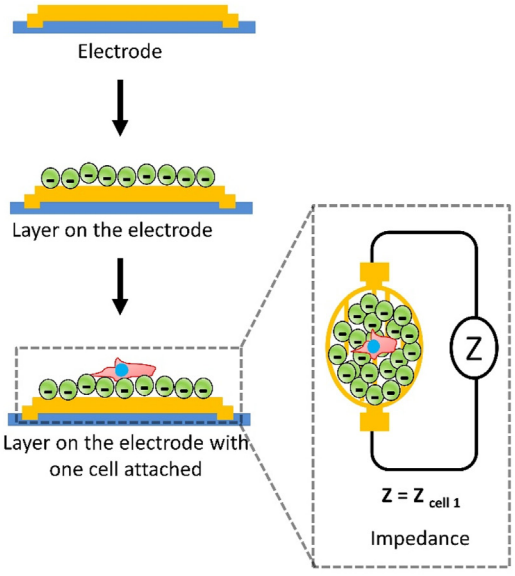

Fig. 4. Schematic of layer deposition on Cell Analyzer (RTCA) xCELLigence instrument.

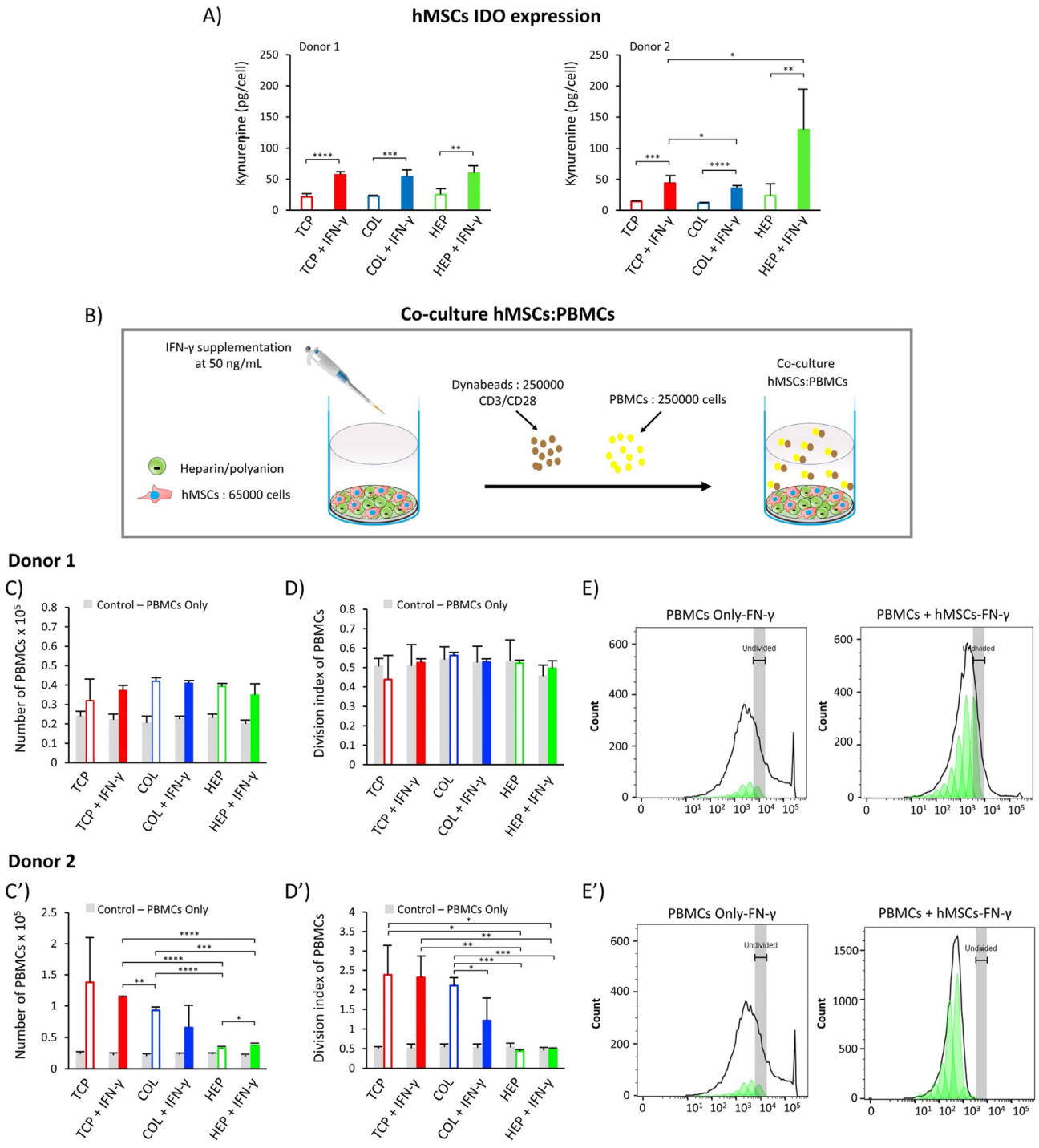

Fig. 5. (A): Cells immunomodulatory potential by IDO activity for hMSCs from two different donors as cultured on TCP, COL-ending, and HEP-ending multilayers with and without IFN-γ. (B): direct-contact co-culture investigations of hMSCs and stimulated PBMCs. (C): The proliferation of PBMCs co-cultured with hMSCs from donor#1. (D): The division index of PBMCs co-cultured with hMSCs from donor#1 (E): peak fit analysis of PBMCs proliferation for donor#1. (C′): The proliferation of PBMCs co-cultured with hMSCs from donor#2. (D′): The division index of PBMCs co-cultured with hMSCs from donor#2 (E′): peak fit analysis of PBMCs proliferation for donor#2. The gray bars reflected the proliferation of only PBMCs cultured in cell medium. Data are presented as the mean ± standard deviation of n = 4 samples. The p-values < 0.05 are represented by *, p-values < 0.01 by **, p-values < 0.001 by *** and p-values < 0.0001 by ****.

COL-ending and HEP-ending multilayers compared to the TCP (p-value< 0.05); in particular, the HEP-ending multilayers with IFN-γ have a higher level of the IDO expression. However, donor#1 shows the same level of the IDO expression for all surfaces containing the IFN-γ. These findings may indicate that IDO expression is related to donor behavior and different donors have different responses [66–68]. In addition, results for both donors show that using the (HEP/COL) multilayers does not decrease the level of IDO activity in reference to the same amount of the IDO expression for the TCP and (HEP/COL) multilayers without IFN-γ. These in vitro studies indicate that the level of IDO depends on not only the different donor's response but also the presence of IFN-γ and the presence of the multilayers. These results are in line with the study done by Cifuentes et al. [29] that showed the IFN-γ is a key regulator of IDO activity. Moreover, pre-treatment of hMSCs with IFN-γ is frequently used

to enhance the cells' immunomodulatory and differentiation activity by activating the expression of IDO [24,69]. However, we have demonstrated that the expression of IDO by hMSCs was higher when cultured on HEP-ending multilayers supplemented with IFN-γ for donor#2. These comply with our previous study, which indicated that HEP-ending multilayers supplemented with IFN-γ can promote the production of cells with pro-inflammatory and immunoregulatory capacities [12]. Therefore, using (HEP/COL) multilayers supplemented with IFN-γ in a culture medium can improve the cell's immunomodulatory activity which may vary donor-to-donor.

3.5. PBMC:hMSC Co-culture

The ability of hMSCs to regulate the proliferation of peripheral blood mononuclear cells (PBMCs) was determined by direct-contact co-culture investigations of hMSCs and stimulated PBMCs. The investigation was conducted for TCP, COL-ending, and HEP-ending multilayers after 3 days post-stimulation with or without IFN-γ supplemented in the cell culture media. In addition, control conditions of PBMCs alone were evaluated on TCP, COL-ending, and HEP-ending with and without IFN-γ. PBMCs with Human T Activator CD3/CD28 Dynabeads (CDs) suspended in hMSCs attached to the surfaces are shown in Supplementary Fig. S1. The proliferation of PBMCs alone (PBMCs seeded in the surface without hMSCs) was not negatively affected by multilayers with or without the IFN-γ supplemented in the cell culture medium, shows in Fig. 5 (C&C′)). This investigation indicates that the proliferation of PBMCs depends neither on the IFN-γ nor the multilayers alone. Regarding the proliferation of PBMCs co-cultured with hMSCs from donor#1, the proliferation of PBMCs shows a slight reduction on TCP without IFN-γ compared to TCP with IFN-γ, which is not statistically significant (Fig. 5 (C)). Also, hMSCs from donor #1 do not suppress PBMCs proliferation and has the same level of proliferation on TCP without IFN-γ, COL-ending, and HEP-ending multilayers with and without IFN-γ. HMSCs from donor #2 treated with IFN- γ are capable of reducing PBMCs proliferation, particularly when cultured on COL-ending multilayers. Donor#2 shows a higher reduction on PBMCs proliferation when hMSCs were cultured with IFN-γ on TCP than without IFN-γ. In addition, donor#2 shows a higher reduction of PBMCs when cultured on HEP-ending. Also, the division index (total number of divisions/the number of cells at the start of culture) has the same trend as the number of PBMCs. Interestingly, peak fit analysis of PBMCs proliferation shows that hMSCs (both donor#1 & donor#2) allowed more generations of PBMCs to proliferate Fig. 5 (E&E′). The results for donor#2 indicate that the presence of IFN-γ in COL-ending multilayers may increase hMSCs suppression capacity of PBMCs proliferation compared to surfaces without IFN-γ which also is related with the donor's behavior. In addition, HEP-ending multilayers may have the ability to suppress PBMCs proliferation for different donors without preactivated with IFN-γ.

Since IDO expression increases in the presence of IFN-γ in culture medium and the response is enhanced by the presence of the multilayers, we confirm that IFN-γ enhances the immunosuppressive potency of hMSCs cultured on HEP/COL coatings. Kwee et al. observed a similar behavior by studying the response to soluble IFN-γ of hMSCs cultured on collagen or fibrin biomaterials [70]. These findings for donor#2 are consistent with the results of [70–72], which confirm the enhancement of hMSCs immunosuppressive potency due to the presence of IFN-γ on COL-ending multilayers. In addition, these results comply with our previous study done by D. Castilla-Casadiego et al. [12] on cytokine expressions on the same multilayers, which suggests that (HEP/COL) multilayers are enhancing the activity of IFN-γ producing pre-activated hMSCs with a higher immunosuppressive capability than those cultured in TCP with soluble IFN-γ. Therefore, we identified that (HEP/COL) multilayers can promote not only immunoregulatory capacities but also the immunosuppression capacities. Kwee et al. suggests that the enhancement in immunosuppressive properties of hMSCs cultured on collagen biomaterials and exposed to soluble IFN-γ may be due to integrin engagement, however the response in strongly dependent on the donors [66]. There is a need to have a better understanding on different donor behavior on (HEP/COL) multilayers.

3.6. hMSC differentiation

After 6 days culture, the ability of hMSCs to differentiate into osteogenic and adipogenic lineages cells was induced by supplementing the growth media with differentiation media to confirm the multipotentiality of hMSCs after IFN- γ exposure and culture on (HEP/COL) multilayers. After about one week of incubation, cell functions associated with osteoblast differentiation (ALP activity, calcium deposition) and adipogenic differentiation were evaluated. To maintain the consistency of all experimental design, we seeded the cells with the regular expansion medium for six days. After that we added the differentiation medium for 7–10 days. Mineralization was also characterized from microscope images. Cell morphologies for long-term culture in normal, osteogenic, and adipogenic medium were evaluated on TCP, COL-ending, and HEP-ending multilayers with and without IFN-γ. Notably, in Fig. 6 (A&B), treatment with IFN-γ had no inhibitory effect on both the osteogenic and adipogenic differentiation of hMSCs. There are large areas visible with red (Alizarin Red staining) and purple (Oil Red staining), indicating the formation of the calcified regions and adipocyte-like cells, respectively.

No staining was observed on cells cultured in regular expansion medium, as shown in Supplementary Fig S2 & S3. Control cells keep their polygonal morphology, which was followed by the loss of contact inhibition to multilayer growth. Fig. 6 (A) shows that cells on TCP expressed only weak staining. However, hMSCs cultured on COL-ending and HEP-ending multilayers showed an increase in the size of calcium deposits formed by the clustering of cells due to the strong staining with Alizarin red, which indicates osteogenic differentiation of cells. The same results were found for donor#2, as shown in Fig. 6 (A′). Increasing the size of red color mineral nodules is a typical feature during osteogenic differentiation of hMSCs [73]. ALP is an enzyme present in bone-related cells and is considered key to mineralization [74]. Its activity is related to the level of inorganic phosphate, a component of the bone mineral phase [75]. Therefore, ALP activity has been considered as an early indicator of osteoblast differentiation. Results for ALP activity are summarized in Fig. 6 (C&C').

Regarding donor#1, multilayers showed enhanced intracellular levels of ALP upon stimulation with IFN-γ as compared to TCP. Also, the TCP, COL-ending, and HEP-ending multilayer surfaces with IFN-γ have higher ALP activity than the surfaces without IFN-γ. In addition, Fig. 6 (C) shows that HEP-ending multilayers have a slightly better cell osteogenic differentiation than COL-ending multilayers, particularly with IFN-γ in culture medium. Similarly, donor#2 shows the same result Fig. 6 (C'). Sabino et al. [76] suggested that this can be attributed to the fact that heparin has the ability to prompt osteogenic differentiation of hMSCs. These in vitro studies indicate that IFN-γ can improve the intercellular level of ALP activity. Also, a study done by C. Lamoury et al. indicated that IFN-γ influences the osteocytic differentiation of both mouse and human MSCs [24]. These findings show that the differentiation of hMSCs treatment with IFN-γ need more studies.

When cells were incubated in the basal adipogenic differentiation medium for seven days, the hMSCs changed from long spindle-shaped to flattened round, or polygonal cells Fig. 6 (B&B'). The undifferentiated hMSCs controls (cultured in hMSCs growth medium) displayed no staining Fig. S2. However, cells show good differentiation on TCP, COL-ending and HEP-ending multilayers not only without IFN-γ but also with IFN-γ. These can indicate that IFN-γ does not suppress cells differentiation.

3.7. Immunophenotype assay

For the differentiation of hMSCs, three differentially expressed CD markers were selected for confirmation by flow cytometry. Expression of

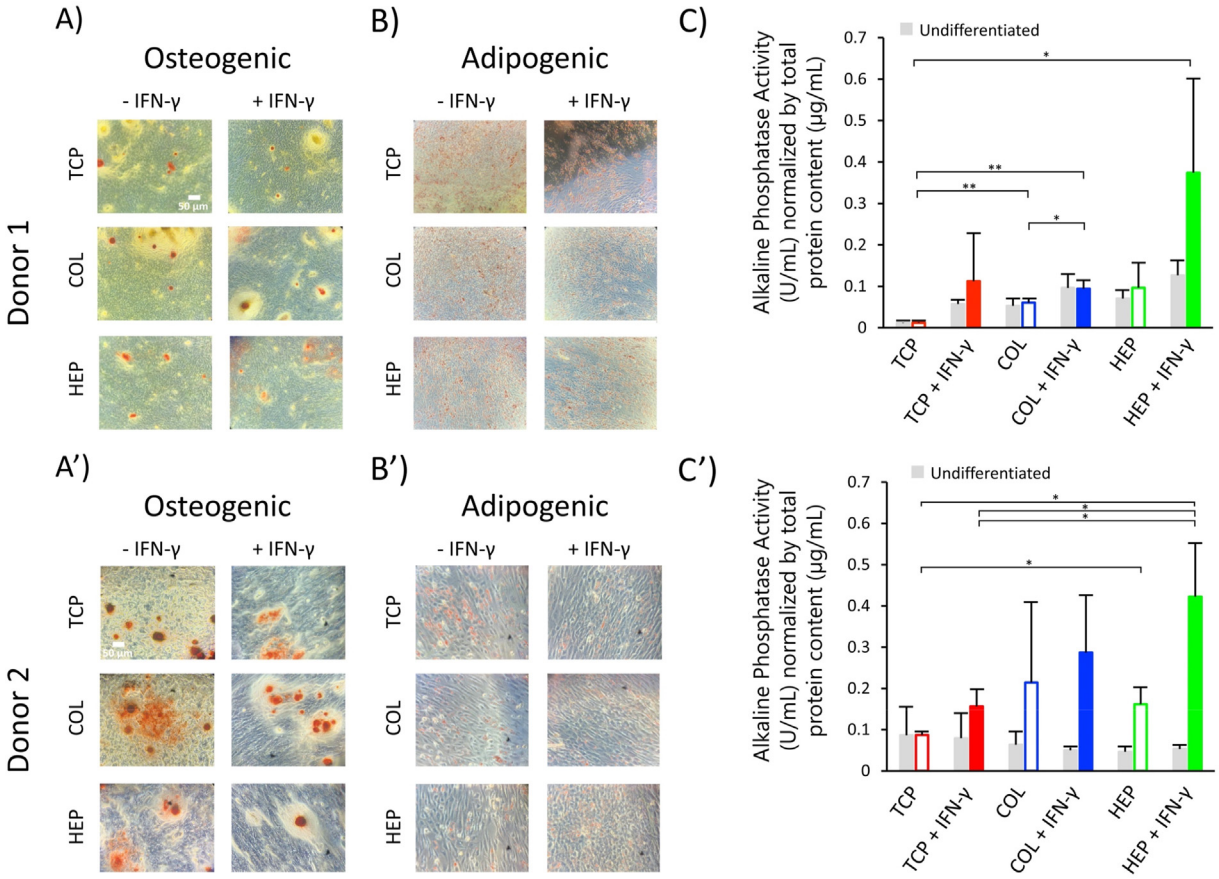

Fig. 6. hMSCs differentiation. (A): Osteogenic differentiated hMSCs from donor#1 were stained using Alizarin Red. (B): Adipogenic differentiated hMSCs from donor#1 were stained using Oil Red. (C): Alkaline phosphatase (ALP) assays were performed after induced osteogenesis on TCP, COL-ending, and HEP-ending multilayers for hMSCs from donor#1. (A′): Osteogenic differentiated hMSCs from donor#2 were stained using Alizarin Red. (B′): Adipogenic differented hMSCs from donor#2 were stained using Oil Red. (C′): Alkaline phosphatase (ALP) assays were performed after of induced osteogenesis on TCP, COL-ending, and HEP-ending multilayers for hMSCs from donor#2. Data are presented as the mean ± standard deviation of n = 4 samples. The p-values < 0.05 are represented by *, p-values < 0.01 by **, p-values < 0.001 by *** and p-values < 0.0001 by ****.

CD10, CD92, and CD105 in hMSCs from two individual donors on TCP, COL-ending, and HEP-ending with and without IFN-γ was analyzed. The study done by C. Granéli et al. suggested that CD10 and CD 92 are surface markers of the osteogenic and adipogenic differentiation [77]. In addition, the expression of the hMSCs-associated CD marker, CD105, was analyzed to evaluate changes in the hMSCs phenotype of the cells during the differentiation process. The expression of CD10 and CD92 were chosen to evaluate the osteogenic and adipogenic differentiation. The median fluorescence intensity MFI ratios (differentiated/undifferentiated) hMSCs for donor#1 and donor#2 are presented in Fig. 7&8.

Regarding donor#1 osteogenic and adipogenic differentiation, the MFI of differentiated cells for CD10 is higher than that of the undifferentiated cells for all surfaces (containing TCP, COL-ending, and HEP-ending multilayers surface with and without IFN-γ) Fig. 7. However, the MFI of differentiated cells for CD92 is slightly less than that of the undifferentiated cells (except for TCP with IFN-γ and HEP-ending multilayers without IFN-γ) Fig. 7. Moreover, the expression of hMSCs marker CD105 was higher in the undifferentiated cells at all surfaces, which means that cells do not differentiate. Regarding donor#2, the same trend for CD10 and CD105 is observed, although the MFI of differentiated cells for CD92 was significantly increased compared with undifferentiated cells. Histograms of CD105, CD10, and CD92 are shown in Fig. 8. CD10 is a cell surface that has been described as a surface marker present on hMSCs isolated from both bone marrow and adipose tissue [78–80]. As a result, an increase in the expression of CD10 shows that more cells differentiate between the osteogenic and adipogenic cells. Also, CD92 is increased in adipogenic hMSCs. Consequently, CD10 and CD92 displayed a higher expression in both osteogenically and adipogenically differentiated hMSCs on all surfaces (TCP, COL-ending, and HEP-ending multilayers surface with and without IFN-γ) compared with an undifferentiated control. These results can indicate that both (HEP/COL) multilayers and IFN-γ do not affect the differentiation and phenotype of the cells.

4. Conclusions

This study demonstrates that polyelectrolyte layers made of heparin and collagen were successfully built up using the layer-by-layer assembly method. QCM-D results demonstrate that the (HEP/COL) multilayers are soft and viscoelastic, and that IFN-γ adsorption depends on the composition of the final layer. Also, (HEP/COL) multilayers present good stability in presence of the IFN-γ. We observed that (HEP/COL) multilayers did not negatively influence the viability, adhesion, proliferation, and differentiation of hMSCs in the presence of soluble IFN-γ. Also, multilayers may lead to improve the anti-proliferation effect of IFN-γ on hMSCs. When CD3/CD28-activated peripheral blood mononuclear cells are co-cultured with hMSCs cultured on (HEP/COL) multilayers, a reduction in PBMC proliferation is observed compared to culture on TCP. In compliance with the present study, other studies demonstrated that the immunosuppression capacity of hMSCs on biomaterials between different donors are corelated to the IDO activity [70]. Our study shows that HEP-ending multilayers was the surface that offered a greater stimulation on the IDO expression, and PBMCs suppression. Though

Osteogenic

A)

MFI Ratio (Osteogenic differentiated /undifferentiated)

CD Markers \ Conditions	- IFN-γ			+ IFN-γ		
	TCP	COL	HEP	TCP	COL	HEP
CD 105	0.56	0.54	0.62	0.4	0.52	0.41
CD 10	1.76	1.95	2.18	1.04	2.03	0.95
CD 92	0.82	1	0.95	0.69	1.31	0.86

B)

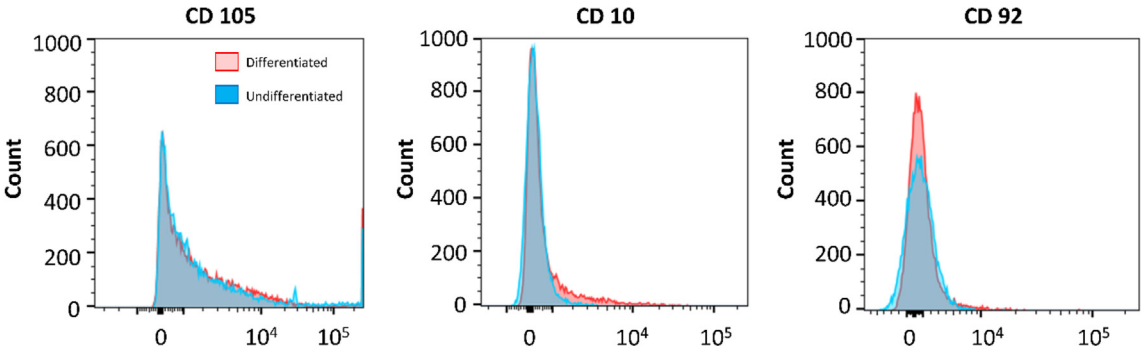

Adipogenic

A)

MFI Ratio (Adipogenic differentiated /undifferentiated)

CD Markers \ Conditions	- IFN-γ			+ IFN-γ		
	TCP	COL	HEP	TCP	COL	HEP
CD 105	0.72	0.54	0.007	0.16	0.58	0.4
CD 10	1.47	1.34	0.38	0.11	1.9	1.27
CD 92	0.88	1.27	0.28	0.11	1.83	1.09

B)

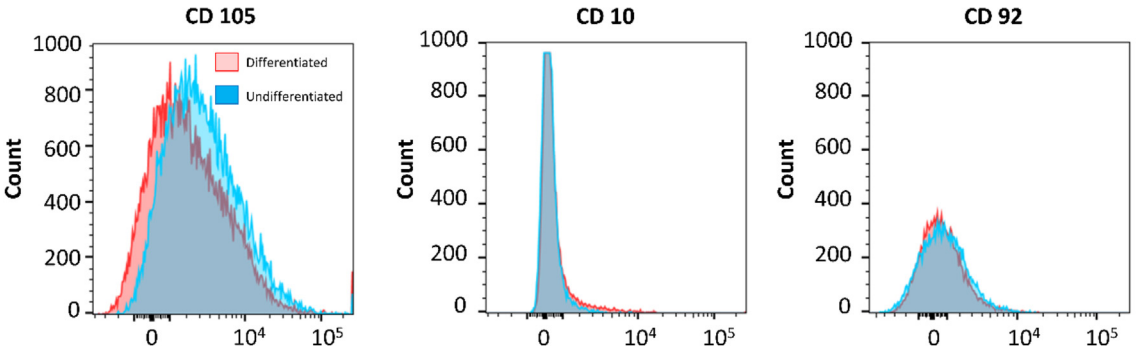

Fig. 7. Flow cytometry of hMSCs from donor#1, Top (Osteogenic) (A): MFI ratios between osteogenically differentiated and undifferentiated hMSCs. (B): Histograms of CD105, CD10 and CD92. Bottom (Adipogenic) (A): MFI ratios between adipogenically differentiated and undifferentiated hMSCs. (B): Histograms of CD 105, CD10, and CD92.

Osteogenic

A)

MFI Ratio (Osteogenic differentiated /undifferentiated)

CD Markers \ Conditions	- IFN-γ			+ IFN-γ		
	TCP	COL	HEP	TCP	COL	HEP
CD 105	1.08	0.71	3.3	1.4	1.105	1.25
CD 10	8.89	12.06	3.76	8.54	14.05	3.42
CD 92	21.4	3.01	1.95	15.12	17.88	13.9

B)

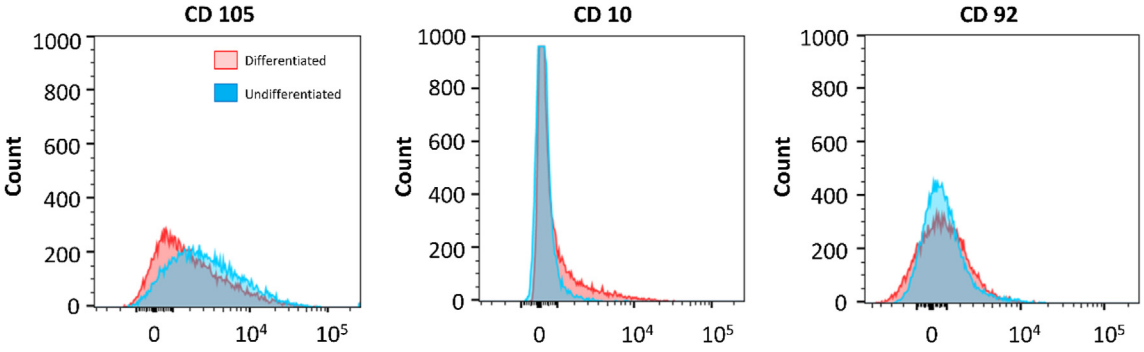

Adipogenic

A)

MFI Ratio (Adipogenic differentiated /undifferentiated)

CD Markers \ Conditions	- IFN-γ			+ IFN-γ		
	TCP	COL	HEP	TCP	COL	HEP
CD 105	0.48	0.44	1.61	0.98	0.7	0.74
CD 10	6.85	7.81	2.75	7.66	9.42	2.49
CD 92	15.35	3.01	2.003	11.79	13.09	14.48

B)

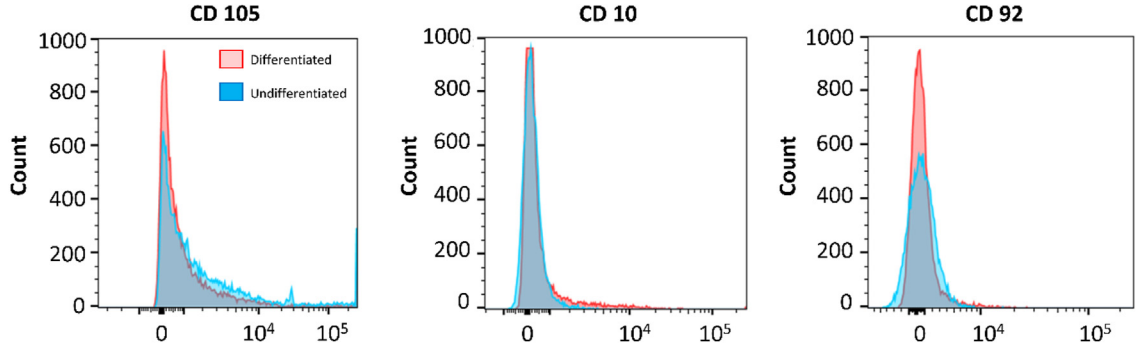

Fig. 8. Flow cytometry of hMSCs from donor#2. Top (Osteogenic_Backspace) (A): MFI ratios between osteogenically differentiated and undifferentiated hMSCs. (B): Histograms of CD105, CD10 and CD92. Bottom (Adipogenic) (A): MFI ratios between adipogenically differentiated and undifferentiated hMSCs. (B): Histograms of CD105, CD10, and CD92.

different responses were observed for the two donors evaluated. This study shows that (HEP/COL) multilayers can modulate hMSCs response to soluble factors, improving the immunosuppressive potential of hMSCs which may lead to more efficient cell manufacturing without additional expenses in the manufacturing process and produce a better-quality cell product. (HEP/COL) multilayers can be applied to any surface including bioreactors or microcarriers which can be used to culture hMSCs meant for cell-based therapies aimed at treating several immune diseases.

Author contributions

Mahsa Haseli and David A. Castilla-Casadiego: Methodology, writing-original draft preparation, visualization, formal analysis, data curation, investigation. Luis Pinzon-Herrera, Alexander Hillsley, Katherine A. Miranda-Muñoz, Srikanth Sivaraman: Data curation. Adrianne M. Rosales, Raj R. Rao: Writing-reviewing and editing, resources. Jorge Almodovar: Conceptualization, supervision, writing-reviewing and editing, resources, funding acquisition, project administration.

Declaration of competing interest

The authors declare that they have no known competing financial interests or personal relationships that could have appeared to influence the work reported in this paper.

Acknowledgement

This work was financially supported in part by the National Science Foundation under grant no. 2051582, by the Arkansas Bioscience Institute, and by the "Programa de Apoyo Institucional Para la Formación en Estudios de Posgrados en Maestrías y Doctorados de La Universidad del Atlántico, Colombia" by providing DCC a scholarship. The authors greatly appreciate the Arkansas Nano & Biomaterials Characterization Facility for help with the use of the XPS. Additionally, the authors thank Integra Life Sciences for their generous donation of lyophilized Type I Collagen. The authors greatly appreciate Dr. Greenlee and Sergio Ivan Perez Bakovic from the University of Arkansas for equipment access and help during quartz crystal microbalance (QCM) measurements.

Supporting information

Microscopy images of PBMCs with Human T Activator CD3/CD28 Dynabeads (CDs) suspended in hMSCs attached to the surfaces, and images of hMSCs cultured in regular expansion media stained with Alizarin Red and Oil-red O as control.

Appendix A. Supplementary data

Supplementary data to this article can be found online at https://doi.org/10.1016/j.mtbio.2021.100194.

References

[1] T.L. Ramos, et al., MSC surface markers (CD44, CD73, and CD90) can identify human MSC-derived extracellular vesicles by conventional flow cytometry, Cell Commun. Signal. 14 (1) (2016) 1–14, https://doi.org/10.1186/s12964-015-0124-8.

[3] Y.P. Rubtsov, Y.G. Suzdaltseva, K.V. Goryunov, N.I. Kalinina, V.Y. Sysoeva, V.A. Tkachuk, Regulation of immunity via multipotent mesenchymal stromal cells, Acta Naturae 4 (1) (2012) 23–31, https://doi.org/10.32607/20758251-2012-4-1-23-31.

[4] K. Suzuki, N. Chosa, S. Sawada, N. Takizawa, T. Yaegashi, A. Ishisaki, Enhancement of anti-inflammatory and osteogenic abilities of mesenchymal stem cells via cell-to-cell adhesion to periodontal ligament-derived fibroblasts, Stem Cell. Int. 2017 (2017), https://doi.org/10.1155/2017/3296498.

[5] R.E. Newman, D. Yoo, M.A. LeRoux, A. Danilkovitch-Miagkova, Treatment of inflammatory diseases with mesenchymal stem cells, Inflamm. Allergy - Drug Targets 8 (2) (2009) 110–123, https://doi.org/10.2174/187152809788462635.

[6] A. Uccelli, L. Moretta, V. Pistoia, Mesenchymal stem cells in health and disease, Nat. Rev. Immunol. 8 (9) (2008) 726–736, https://doi.org/10.1038/nri2395.

[7] F. Gao, et al., Mesenchymal stem cells and immunomodulation: current status and future prospects, Cell Death Dis. 7 (1) (2016), https://doi.org/10.1038/cddis.2015.327.

[8] P.S. Frenette, S. Pinho, D. Lucas, C. Scheiermann, Mesenchymal Stem Cell: Keystone of the Hematopoietic Stem Cell Niche and a Stepping-Stone for Regenerative Medicine, vol. 31, 2013.

[9] Y. Wang, X. Chen, W. Cao, Y. Shi, Plasticity of mesenchymal stem cells in immunomodulation: pathological and therapeutic implications, Nat. Immunol. 15 (11) (2014) 1009–1016, https://doi.org/10.1038/ni.3002.

[10] J.A. Ankrum, J.F. Ong, J.M. Karp, Mesenchymal stem cells: immune evasive, not immune privileged, Nat. Biotechnol. 32 (3) (2014) 252–260, https://doi.org/10.1038/nbt.2816.

[11] R.R. Sharma, K. Pollock, A. Hubel, D. McKenna, Mesenchymal stem or stromal cells: a review of clinical applications and manufacturing practices, Transfusion 54 (5) (2014) 1418–1437, https://doi.org/10.1111/trf.12421.

[12] D.A. Castilla-Casadiego, J.R. García, A.J. García, J. Almodovar, Heparin/collagen coatings improve human mesenchymal stromal cell response to interferon gamma, ACS Biomater. Sci. Eng. 5 (6) (2019) 2793–2803, https://doi.org/10.1021/acsbiomaterials.9b00008.

[13] J. Cuerquis, et al., Human mesenchymal stromal cells transiently increase cytokine production by activated T cells before suppressing T-cell proliferation: effect of interferon-γ and tumor necrosis factor-α stimulation, Cytotherapy 16 (2) (2014) 191–202, https://doi.org/10.1016/j.jcyt.2013.11.008.

[14] T.J. Kean, P. Lin, A.I. Caplan, J.E. Dennis, MSCs: delivery routes and engraftment, cell-targeting strategies, and immune modulation, Stem Cell. Int. 2013 (2013), https://doi.org/10.1155/2013/732742.

[15] T. Asami, et al., Modulation of murine macrophage TLR7/8-mediated cytokine expression by mesenchymal stem cell-conditioned medium, Mediat. Inflamm. 2013 (2013), https://doi.org/10.1155/2013/264260.

[16] Y. Zhang, et al., Exosomes derived from mesenchymal stromal cells promote axonal growth of cortical neurons, Mol. Neurobiol. 54 (4) (2017) 2659–2673, https://doi.org/10.1007/s12035-016-9851-0.

[17] M. Khan, Human mesenchymal stem cells, Hum. Mesenchymal Stem Cells 1416 (Cmc) (2021) 1–127, https://doi.org/10.1016/s0141-0229(97)83511-9.

[18] A. Gebler, O. Zabel, B. Seliger, The immunomodulatory capacity of mesenchymal stem cells, Trends Mol. Med. 18 (2) (2012) 128–134, https://doi.org/10.1016/j.molmed.2011.10.004.

[19] G. Ren, et al., Mesenchymal stem cell-mediated immunosuppression occurs via concerted action of chemokines and nitric oxide, Cell Stem Cell 2 (2) (2008) 141–150, https://doi.org/10.1016/j.stem.2007.11.014.

[20] M. Krampera, et al., Role for interferon-γ in the immunomodulatory activity of human bone marrow mesenchymal stem cells, Stem Cell. 24 (2) (2006) 386–398, https://doi.org/10.1634/stemcells.2005-0008.

[21] M.W. Klinker, R.A. Marklein, J.L. Lo Surdo, C.H. Wei, S.R. Bauer, Morphological features of IFN-γ-stimulated mesenchymal stromal cells predict overall immunosuppressive capacity, Proc. Natl. Acad. Sci. U. S. A 114 (13) (2017) E2598–E2607, https://doi.org/10.1073/pnas.1617933114.

[22] J.N.M. Ijzermans, R.L. Marquet, Interferon-gamma: a review, Immunobiology 179 (4–5) (1989) 456–473, https://doi.org/10.1016/S0171-2985(89)80049-X.

[23] Y. Liu, et al., Mesenchymal stem cell-based tissue regeneration is governed by recipient T lymphocytes via IFN-γ and TNF-α, Nat. Med. 17 (12) (2011) 1594–1601, https://doi.org/10.1038/nm.2542.

[24] J. Croitoru-Lamoury, et al., Interferon-γ regulates the proliferation and differentiation of mesenchymal stem cells via activation of indoleamine 2,3 dioxygenase (IDO), PLoS One 6 (2) (2011), https://doi.org/10.1371/journal.pone.0014698.

[25] M.O. Dellacherie, B.R. Seo, D.J. Mooney, Macroscale biomaterials strategies for local immunomodulation, Nat. Rev. Mater. 4 (6) (2019) 379–397, https://doi.org/10.1038/s41578-019-0106-3.

[26] R.S. Tuan, G. Boland, R. Tuli, Adult mesenchymal stem cells and cell-based tissue engineering, Arthritis Res. Ther. 5 (1) (2003) 32–45, https://doi.org/10.1186/ar614.

[27] R.A. Marklein, M.W. Klinker, K.A. Drake, H.G. Polikowsky, E.C. Lessey-Morillon, S.R. Bauer, Morphological profiling using machine learning reveals emergent subpopulations of interferon-γ–stimulated mesenchymal stromal cells that predict immunosuppression, Cytotherapy 21 (1) (2019) 17–31, https://doi.org/10.1016/j.jcyt.2018.10.008.

[28] R.A. Marklein, J. Lam, M. Guvendiren, K.E. Sung, S.R. Bauer, Functionally-relevant morphological profiling: a tool to assess cellular heterogeneity, Trends Biotechnol. 36 (1) (2018) 105–118, https://doi.org/10.1016/j.tibtech.2017.10.007.

[29] S.J. Cifuentes, P. Priyadarshani, D.A. Castilla-Casadiego, L.J. Mortensen, J. Almodóvar, M. Domenech, Heparin/collagen surface coatings modulate the growth, secretome, and morphology of human mesenchymal stromal cell response to interferon-gamma, *J. Biomed. Mater. Res. Part A*, no. March (2020) 1–15, https://doi.org/10.1002/jbm.a.37085.

[30] V. Gribova, R. Auzely-Velty, C. Picart, Polyelectrolyte multilayer assemblies on materials surfaces: from cell adhesion to tissue engineering, Chem. Mater. 24 (5) (2012) 854–869, https://doi.org/10.1021/cm2032459.

[31] C. Picart, et al., Primary cell adhesion on RGD-functionalized and covalently crosslinked thin polyelectrolyte multilayer films, Adv. Funct. Mater. 15 (1) (2005) 83–94, https://doi.org/10.1002/adfm.200400106.

[32] C. Picart, Polyelectrolyte multilayer films: from physico-chemical properties to the control of cellular processes, Curr. Med. Chem. 15 (7) (2008) 685–697, https://doi.org/10.2174/092986708783885219.
[33] P. Gentile, I. Carmagnola, T. Nardo, V. Chiono, Layer-by-layer assembly for biomedical applications in the last decade, Nanotechnology 26 (42) (2015), 422001, https://doi.org/10.1088/0957-4484/26/42/422001.
[34] D.L. Kusindarta, H. Wihadmadyatami, The Role of Extracellular Matrix in Tissue Regeneration, Tissue Regen. (2018), https://doi.org/10.5772/intechopen.75728.
[35] G.A. Di Lullo, S.M. Sweeney, J. Körkkö, L. Ala-Kokko, J.D. San Antonio, Mapping the ligand-binding sites and disease-associated mutations on the most abundant protein in the human, type I collagen, J. Biol. Chem. 277 (6) (2002) 4223–4231, https://doi.org/10.1074/jbc.M110709200.
[36] M.S. Douglas, D.A. Rix, J.H. Dark, D. Talbot, J.A. Kirby, Examination of the mechanism by which heparin antagonizes activation of a model endothelium by interferon-gamma (IPN-γ), Clin. Exp. Immunol. 107 (3) (1997) 578–584, https://doi.org/10.1046/j.1365-2249.1997.3141206.x.
[37] S. Sarrazin, D. Bonnaffé, A. Lubineau, H. Lortat-Jacob, Heparan sulfate mimicry: a synthetic glycoconjugate that recognizes the heparin domain of interferon-γ inhibits the cytokine activity, J. Biol. Chem. 280 (45) (2005) 37558–37564, https://doi.org/10.1074/jbc.M507729200.
[38] D.A. Castilla-Casadiego, L. Pinzon-Herrera, M. Perez-Perez, B.A. Quiñones-Colón, D. Suleiman, J. Almodovar, Simultaneous characterization of physical, chemical, and thermal properties of polymeric multilayers using infrared spectroscopic ellipsometry, Colloids Surf. A Physicochem. Eng. Asp. 553 (2018) 155–168, https://doi.org/10.1016/j.colsurfa.2018.05.052.
[39] L. Pinzon-Herrera, J. Mendez-Vega, A. Mulero-Russe, D.A. Castilla-Casadiego, J. Almodovar, Real-time monitoring of human Schwann cells on heparin-collagen coatings reveals enhanced adhesion and growth factor response, J. Mater. Chem. B 8 (38) (2020) 8809–8819, https://doi.org/10.1039/d0tb01454k.
[40] D.A. Castilla-Casadiego, H. Timsina, M. Haseli, L. Pinzon-Herrera, Y.H. Chiao, S.R. Wickramasinghe, J. Almodovar, Methods for the assembly and characterization of polyelectrolyte multilayers as microenvironments to modulate human mesenchymal stromal cell response, ACS Biomater. Sci. Eng. 6 (12) (2020) 6626–6651, https://doi.org/10.1021/acsbiomaterials.0c01397.
[41] D.A. Castilla-Casadiego, A.M. Reyes-Ramos, M. Domenech, J. Almodovar, Effects of physical, chemical, and biological stimulus on h-MSC expansion and their functional characteristics, Ann. Biomed. Eng. 48 (2) (2020) 519–535, https://doi.org/10.1007/s10439-019-02400-3.
[43] A. Bertolo, D. Pavlicek, A. Gemperli, M. Baur, T. Pötzel, J. Stoyanov, Increased motility of mesenchymal stem cells is correlated with inhibition of stimulated peripheral blood mononuclear cells in vitro, J. Stem Cells Regen. Med. 13 (2) (2017) P62–P74, https://doi.org/10.46582/jsrm.1302010.
[44] L. Boland, A.J. Burand, A.J. Brown, D. Boyt, V.A. Lira, J.A. Ankrum, IFN-γ and TNF-α pre-licensing protects mesenchymal stromal cells from the pro-inflammatory effects of palmitate, Mol. Ther. 26 (3) (2018) 860–873, https://doi.org/10.1016/j.ymthe.2017.12.013.
[45] M.C. Killer, et al., Immunosuppressive capacity of mesenchymal stem cells correlates with metabolic activity and can be enhanced by valproic acid, Stem Cell Res. Ther. 8 (1) (2017) 1–8, https://doi.org/10.1186/s13287-017-0553-y.
[46] K.A. Marx, Quartz crystal microbalance: a useful tool for studying thin polymer films and complex biomolecular systems at the solution - surface interface, Biomacromolecules 4 (5) (2003) 1099–1120, https://doi.org/10.1021/bm020116i.
[47] C.D. Easton, A.J. Bullock, G. Gigliobianco, S.L. McArthur, S. Macneil, Application of layer-by-layer coatings to tissue scaffolds-development of an angiogenic biomaterial, J. Mater. Chem. B 2 (34) (2014) 5558–5568, https://doi.org/10.1039/c4tb00448e.
[48] Q. Lin, J. Yan, F. Qiu, X. Song, G. Fu, J. Ji, Heparin/collagen multilayer as a thromboresistant and endothelial favorable coating for intravascular stent, J. Biomed. Mater. Res. 96 A (1) (2011) 132–141, https://doi.org/10.1002/jbm.a.32820.
[49] I. Reviakine, D. Johannsmann, R.P. Richter, Hearing what you cannot see and visualizing what you hear: interpreting quartz crystal microbalance data from solvated interfaces, Anal. Chem. 83 (23) (2011) 8838–8848, https://doi.org/10.1021/ac201778h.
[50] S. Boddohi, J. Almodóvar, H. Zhang, P.A. Johnson, M.J. Kipper, Layer-by-layer assembly of polysaccharide-based nanostructured surfaces containing polyelectrolyte complex nanoparticles, Colloids Surf. B Biointerfaces 77 (1) (2010) 60–68, https://doi.org/10.1016/j.colsurfb.2010.01.006.
[51] Q. Lin, J. Yan, F. Qiu, X. Song, G. Fu, J. Ji, Heparin/collagen multilayer as a thromboresistant and endothelial favorable coating for intravascular stent, J. Biomed. Mater. Res. 96 A (1) (2011) 132–141, https://doi.org/10.1002/jbm.a.32820.
[52] D.S. Salloum, S.G. Olenych, T.C.S. Keller, J.B. Schlenoff, Vascular smooth muscle cells on polyelectrolyte multilayers: hydrophobicity-directed adhesion and growth, Biomacromolecules 6 (1) (2005) 161–167, https://doi.org/10.1021/bm0497015.
[53] K. Zhang, D. Huang, Z. Yan, C. Wang, Heparin/collagen encapsulating nerve growth factor multilayers coated aligned PLLA nanofibrous scaffolds for nerve tissue engineering, J. Biomed. Mater. Res. 105 (7) (2017) 1900–1910, https://doi.org/10.1002/jbm.a.36053.
[54] A.M. Ferreira, P. Gentile, S. Toumpaniari, G. Ciardelli, M.A. Birch, Impact of collagen/heparin multilayers for regulating bone cellular functions, ACS Appl. Mater. Interfaces 8 (44) (2016) 29923–29932, https://doi.org/10.1021/acsami.6b09241.
[55] D. Li, et al., Chitosan and collagen layer-by-layer assembly modified oriented nanofibers and their biological properties, Carbohydr. Polym. 254 (2020), 117438, https://doi.org/10.1016/j.carbpol.2020.117438. July 2020.
[56] J. Almodóvar, S. Bacon, J. Gogolski, J.D. Kisiday, M.J. Kipper, Polysaccharide-based polyelectrolyte multilayer surface coatings can enhance mesenchymal stem cell response to adsorbed growth factors, Biomacromolecules 11 (10) (2010) 2629–2639, https://doi.org/10.1021/bm1005799.
[57] H.M. Wobma, M.A. Tamargo, S. Goeta, L.M. Brown, R. Duran-Struuck, G. Vunjak-Novakovic, The Influence of Hypoxia and IFN-γ on the Proteome and Metabolome of Therapeutic Mesenchymal Stem Cells, vol. 167, Elsevier, 2018.
[58] J. Du, et al., The different effects of IFN-β and IFN-γ on the tumor-suppressive activity of human amniotic fluid-derived mesenchymal stem cells, Stem Cell. Int. 2019 (2019), https://doi.org/10.1155/2019/4592701.
[59] M.H. Hettiaratchi, T. Miller, J.S. Temenoff, R.E. Guldberg, T.C. McDevitt, Heparin microparticle effects on presentation and bioactivity of bone morphogenetic protein-2, Biomaterials 35 (25) (2014) 7228–7238, https://doi.org/10.1016/j.biomaterials.2014.05.011.
[60] S.J. Fritchley, J.A. Kirby, S. Ali, The antagonism of interferon-gamma (IFN-γ) by heparin: examination of the blockade of class II MHC antigen and heat shock protein-70 expression, Clin. Exp. Immunol. 120 (2) (2000) 247–252, https://doi.org/10.1046/j.1365-2249.2000.01178.x.
[61] A. Rezania, K.E. Healy, Biomimetic peptide surfaces that regulate adhesion, spreading, cytoskeletal organization, and mineralization of the matrix deposited by osteoblast-like cells, Biotechnol. Prog. 15 (1) (1999) 19–32, https://doi.org/10.1021/bp980083b.
[62] V. January, RTCA DP Instrument Operator's Manual, ACEA Biosci. Inc (2013) no. January.
[63] J.J. Montesinos, et al., Human bone marrow mesenchymal stem/stromal cells exposed to an inflammatory environment increase the expression of ICAM-1 and release microvesicles enriched in this adhesive molecule: analysis of the participation of TNF-α and IFN-γ, J. Immunol. Res. 2020 (2020) https://doi.org/10.1155/2020/8839625.
[64] O. Takikawa, T. Kuroiwa, F. Yamazaki, R. Kido, Mechanism of interferon-γ action. Characterization of indoleamine 2,3-dioxygenase in cultured human cells induced by interferon -γ and evaluation of the enzyme-mediated tryptophan degradation in its anticellular activity, J. Biol. Chem. 263 (4) (1988) 2041–2048.
[65] W. Däubener, N. Wanagat, K. Pilz, S. Seghrouchni, H.G. Fischer, U. Hadding, A new, simple, bioassay for human IFN-γ, J. Immunol. Methods 168 (1) (1994) 39–47, https://doi.org/10.1016/0022-1759(94)90207-0.
[66] G. Siegel, T. Kluba, U. Hermanutz-Klein, K. Bieback, H. Northoff, R. Schäfer, Phenotype, donor age and gender affect function of human bone marrow-derived mesenchymal stromal cells, BMC Med. 11 (1) (2013), https://doi.org/10.1186/1741-7015-11-146.
[67] O. Katsara, et al., Effects of donor age, gender, and in vitro cellular aging on the phenotypic, functional, and molecular characteristics of mouse bone marrow-derived mesenchymal stem cells, Stem Cell. Dev. 20 (9) (2011) 1549–1561, https://doi.org/10.1089/scd.2010.0280.
[68] T. Wang, J. Zhang, J. Liao, F. Zhang, G. Zhou, Donor genetic backgrounds contribute to the functional heterogeneity of stem cells and clinical outcomes, Stem Cells Transl. Med. 9 (12) (2020) 1495–1499, https://doi.org/10.1002/sctm.20-0155.
[69] M. Science, Tissue engineering and regenerative medicine T issue E ngineering and R egenerative M edicine MicroRNA-146b , a sensitive indicator of mesenchymal stem cell repair of acute renal injury, 2016, pp. 1–10.
[70] K.E.S. Brian, J. Kwee, Johnny Lam, Adovi Akue, Mark A. KuKuruga, K. Zhang, Luo Gu, Functional heterogeneity of IFN- γ – licensed mesenchymal stromal cell immunosuppressive capacity on biomaterials, 2021, pp. 1–12, https://doi.org/10.1073/pnas.2105972118/-/DCSupplemental (Published).
[71] F. Fallarino, U. Grohmann, Using an ancient tool for igniting and propagating immune tolerance: IDO as an inducer and amplifier of regulatory T cell functions, Curr. Med. Chem. 18 (15) (2012) 2215–2221, https://doi.org/10.2174/092986711795656027.
[72] D.S. Kim, et al., Enhanced immunosuppressive properties of human mesenchymal stem cells primed by interferon-γ, EBioMedicine 28 (2018) 261–273, https://doi.org/10.1016/j.ebiom.2018.01.002.
[73] W. Juncheng, et al., High glucose inhibits osteogenic differentiation through the BMP signaling pathway in bone mesenchymal stem cells in mice, EXCLI J. 12 (2009) (2013) 584–597, https://doi.org/10.17877/DE290R-7335.
[74] A. Zhu, M. Zhang, J. Wu, J. Shen, Covalent immobilization of chitosan/heparin complex with a photosensitive hetero-bifunctional crosslinking reagent on PLA surface $ 23 (2002) 4657–4665.
[75] A.M.M. Renata Francielle Bombaldi de Souza, Fernanda Carla Bombaldi de Souza, Andrea Thorpe, Diego Mantovani, Ketul C. Popat, Phosphorylation of chitosan to improve osteoinduction of chitosan/xanthan-based scaffolds for periosteal tissue engineering, Int. J. Biol. Macromol. (2019), https://doi.org/10.1016/j.ijbiomac.2019.12.004.
[76] R.M. Sabino, G. Mondini, M.J. Kipper, A.F. Martins, K.C. Popat, Tanfloc/heparin polyelectrolyte multilayers improve osteogenic differentiation of adipose-derived stem cells on titania nanotube surfaces, Carbohydr. Polym. 251 (2021), 117079,

https://doi.org/10.1016/j.carbpol.2020.117079. September 2020.
[77] C. Granéli, et al., Novel markers of osteogenic and adipogenic differentiation of human bone marrow stromal cells identified using a quantitative proteomics approach, Stem Cell Res. 12 (1) (2014) 153–165, https://doi.org/10.1016/j.scr.2013.09.009.
[78] V. Michel, M. Bakovic, The solute carrier 44A1 is a mitochondrial protein and mediates choline transport, Faseb. J. 23 (8) (2009) 2749–2758, https://doi.org/10.1096/fj.08-121491.
[79] L. Ding, et al., CD10 expression identifies a subset of human perivascular progenitor cells with high proliferation and calcification potentials, Stem Cell. 38 (2) (2020) 261–275, https://doi.org/10.1002/stem.3112.
[80] E.A. Jones, et al., Isolation and characterization of bone marrow multipotential mesenchymal progenitor cells, Arthritis Rheum. 46 (12) (2002) 3349–3360, https://doi.org/10.1002/art.10696.